23rd IAHR International Symposium on Ice
Ann Arbor, Michigan, USA, May 31 to June 3, 2016

Preliminary Calibration of a Rheological Sea Ice Model for Wave-In-Ice using Field Data

Sukun Cheng[1,*], Xin Zhao[1], W. Erick Rogers [2], Jim Thomson[3], Hayley H. Shen[1]
1) Dept. Civil & Env. Eng., Clarkson University,8 Clarkson Ave, Potsdam, NY, USA
2) Naval Research Laboratory (Oceanography Division) Stennis Space Center, MS, USA
3) Applied Physics Laboratory, Civil & Env. Eng., Univ. Washington, Seattle, WA, USA
**) Corresponding author: chengs@clarkson.edu*

A viscoelastic sea ice model has been adopted in the ocean wave model - WAVEWATCH III® to account for the sea ice effect on wave attenuation. The model has two parameters: the effective elasticity G and effective viscosity ν, to describe various types of ice covers. In this study, G, ν are calibrated with the data collected in the Arctic marginal ice zone, during Sep. 30-Nov. 9, 2015. The field conditions and datasets collected are reported in another paper at this symposium (Shen et al.). In this paper, we report the preliminary results of using these data to calibrate the viscoelastic model. The calibrations are done based on two approaches. One approach assumes that sea ice damping is the only factor that modifies the wave energy. The model parameters G, ν are thus calibrated using the corresponding dispersion relation with measured change of wave energy between two buoys. In a real ocean environment, other source terms, such as wind, nonlinear wave-wave interaction and wave dissipation, are present. Therefore, a second approach is also adopted in which the comprehensive wave energy balance equation is used to account for these other source terms. In this paper, we report some preliminary results of these two calibration approaches using a recent field data.

1. Introduction

In polar regions, wave propagation is affected by different types of ice covers. Due to the increase of open water and intensified storm activities (Thomson and Rogers, 2014), there is a strong need to include ice effects in wave models. In this paper, we present a preliminary study of calibrating a viscoelastic model (Wang and Shen, 2010) for ice covers, using data obtained in a recent field experiment (Shen et al., in this Proceedings). This model has been adopted as one of the choices in WAVEWATCH III® to account for the sea ice effect on wave attenuation and wave speed change. This model is chosen because it synthesizes three classic models: mass loading, thin-elastic, and pure viscous. Two calibration approaches are used to inversely determine two rheological parameters in the viscoelastic model. This analysis is preliminary because the wave and ice data used here are still being refined. Furthermore, there are other viscoelastic models that may also be adopted (Mosig et al. 2015). The results presented here thus represent an on-going effort.

The viscoelastic model to be calibrated in this study is briefly summarized first. In this model, the dispersion relation provides the complex wave number $k = k_r + ik_i$, once the angular frequency ω, the ice thickness h, and its rheological properties are given. The real part of the wave number k_r is related to the celerity and the group velocity. Since the wave profile $\eta \sim e^{i(kx-\omega t)} = e^{-k_i x} e^{i(k_r x-\omega t)}$, the imaginary part of the wave number k_i represents an exponential decay of the wave amplitude. The derivation of this model is given in Wang and Shen (2010). This model assumes that a general ice cover may be represented by a Voigt continuum, with two rheological parameters: equivalent shear modulus G and equivalent kinematic viscosity ν. The complete analytical form of the dispersion relation is (Zhao and Shen, 2015):

$$J(\omega^2 - Q_c g k \tanh kH) \frac{\omega^2}{\nu_e^2} \frac{\rho_2}{\rho_1} \frac{1}{\tanh kH} = 0 \qquad [1]$$

with

$$J = gk(4k^3 \alpha \nu_e^2 S_k C_\alpha + N^2 S_\alpha C_k - gk S_k S_\alpha),$$

$$Q_c = 1 + \frac{\rho_1}{\rho_2} \frac{(g^2k^2 - N^4 - 16k^6\alpha^2\nu_e^2)\, S_k S_\alpha - 8k^3 \alpha \nu_e^2\, N^2 (C_\alpha C_k - 1)}{J}$$

where g is the gravitational acceleration, H is water depth, h is the ice thickness, ρ_1 and ρ_2 are the density of ice and water, respectively; $S_k = \sinh(kh)$, $S_\alpha = \sinh(\alpha h)$, $C_k = \cosh(kh)$, $C_\alpha = \cosh(\alpha h)$, $N = \omega + 2ik^2\nu_e$. For a set of ω, h, H, G and ν, multiple k values are solved from the dispersion relation. One of the roots contained in J is shown to correspond to a shear wave with negligible energy (Zhao and Shen, 2015). One of root contained in $\omega^2 - Q_c g k \tanh kH$ relates to the most energetic wave mode. This root is chosen for calibrating the rheological parameters G, ν in this paper.

2. Wave energy balance equation

The wave spectrum evolution is described by the energy balance equation. In deep water and without currents:

$$\frac{\partial F(f,\theta)}{\partial t} + \boldsymbol{c_g} \cdot \nabla_{\mathbf{x}} F(f,\theta) = S_{in} + S_{ds} + S_{nl} \qquad [2]$$

where $F(f,\theta)$ is the spectral energy density, $\boldsymbol{c_g}$ is the group velocity, C is the ice concentration, S_{in} is the wind input term, S_{ds} is the wave dissipation term, mostly through wave breaking, S_{nl} is the energy transfer due to nonlinear interactions among spectral components.

For an ice covered ocean, Eq. [2] should be modified by adding an ice induced source term on the right hand side. Furthermore, as described in the user manual and system documentation (Tolman, 2014). S_{ice} is scaled by the ice concentration *C*, and S_{in} and S_{ds} are scaled by $(1-C)$. Thus, with x being the wave propagation direction, Eq. [2] is simplified to:

$$\frac{\partial c_g F(f,\theta)}{\partial x} = (1-C)(S_{in}+S_{ds}) + S_{nl} + CS_{ice} \quad [3]$$

In the above, steady state is considered. We thus will use only the part of the wave record that is relatively constant in time. We present two calibration methods below based on Eq. [3].

3. Data processing

Several wave measurements were conducted during the R/V Sikuliaq cruise in the western Arctic Ocean from Oct.1 to Nov. 10, 2015. These measurements lasted from hours to 3 days in the marginal ice zone. Three types of buoys were used to record the wave propagation under ice covers. We select some datasets collected by SWIFT (Surface Wave Instrument Floats with Tracking) buoys for the present study. The property of SWIFT buoys and data processing to obtain the directional spectra may be found in Thomson (2012).

The SWIFT data provide wave spectrum, $S(f,t)$, over time intervals about 10-12 minutes. To reduce noise, these $S(f,t)$ records were first smoothed by time average of a selected range, and then moving averaged in the frequency space with 5 adjacent frequencies, to obtain $\bar{S}(f)$. Directional wave spectra $F(f,\theta)$ was derived using $\bar{S}(f)$ and the smoothed directional moments (a_1, a_2, b_1, b_2) by Maximum Entropy Method (Lygre and Krogstad, 1986).

Attenuation rate of wave energy between two buoys in the MIZ $\alpha(f)$ was calculated and used to calibrate the viscoelastic sea ice model later. The calculation of $\alpha(f)$ was based on the wave energy decay over distance between two chosen buoys. We assume that the wave energy decays exponentially between buoys A and B. A duration of one to two hours of relatively steady wave condition was selected. The lead buoy, A, is determined by the larger significant wave height H_s over the whole frequency space, where $H_s = 4\sqrt{\int_0^\infty \bar{S}(f)df}$. Since each frequency component has its own direction, the attenuation is determined for each frequency:

$$\alpha(f_j) = \frac{1}{2d\cos\theta_b} ln\left(\frac{F_A(f_j,\theta_j)}{F_B(f_j,\theta_j)}\right) \quad [4]$$

where d is the distance between the two buoys, θ_b is the acute angle between wave direction θ_j and the line connecting two buoys. The line connecting two buoys is determined by their longitude/latitude locations averaged over the duration of our analysis. In this study, we ignore the possibility that for a given frequency, the wave direction θ_j may differ between A and B. θ_j is thus defined using buoy A as $\theta_j = \{\theta | \max F_A(f_j,\theta), 0° \le \theta < 360°)\}$.

Calibration related ice data such as ice concentration C and ice thickness h were not measured by the SWIFT buoys. An on-board visual observation recorded ice data classified as primary, secondary and tertiary types, under the ASSIST (http://www.iarc.uaf.edu/icewatch) protocol during the cruise. We use duration-averaged C, h of the primary type for this calibration. It is noted that this visual observation was not the in-situ ice condition next to the buoys, since after deployment the ship moved away while the buoys drifted on their own. But because the wave attenuation between two buoys was the result of the regional ice condition, the areal and temporal averaged ice data from these visual observations were reasonable to use.

4. Simple model: $\boldsymbol{S = S_{ice}}$

In this calibration approach, henceforth called the "simple model", we consider S_{ice} as the only source term for wave damping. S_{in}, S_{ds} and S_{nl} are removed from Eq. [3]. We further assume that the group velocity is relatively constant between the two buoys. It yields,

$$c_g \frac{\partial F(f,\theta)}{\partial x} = C S_{ice} \quad [5]$$

Again, assuming an exponential change of attenuation rate of wave energy, we have

$$\frac{\partial F(f_j,\theta_j)}{\partial x} = -2\alpha\left(f_j, \theta_j, G, \nu\right)F \quad [6]$$

The ice induced energy dissipation from the WAVEWATCH III® model (Tolman, 2014) is,

$$S_{ice} = -2c_g k_i(f, G, \nu)F \quad [7]$$

Without direct measurement of the wave speed or wavelength, we assume that group velocity $c_g = d\omega/dk_r$ is the one under ice cover with k_r calculated through the viscoelastic model.

Substituting Eqs. [6,7] into Eq. [5] yields,

$$\alpha(f_j) = C k_i(f_j, G, \nu) \quad [8]$$

The effective shear modulus G and effective kinematic viscosity ν are calibrated resulting in the best fit of Ck_i from the viscoelastic model with the measured data α over the whole wave frequency space, i.e. $\min_{G,\nu}\|\alpha - Ck_i\|_2$. The optimization is done by using the Levenberg-Marquardt algorithm.

5. Full model: $\boldsymbol{S = (1 - C)(S_{in} + S_{ds}) + S_{nl} + CS_{ice}}$

Although sea ice usually dominates wave energy decay, other source terms: wind input S_{in}, wave dissipation S_{ds} and nonlinear wave-wave interaction S_{nl}, may be important in stormy conditions (Li et al., 2015). In which case, we need to consider the full energy balance equation

$$c_g \frac{\partial F(f,\theta)}{\partial x} = -2c_g \alpha F(f,\theta) \ = (1 - C)(S_{in} + S_{ds}) + S_{nl} + CS_{ice} \quad [9]$$

In this paper, the wind input S_{in} and wave dissipation S_{ds} are calculated using formulations from Snyder et al. (1981) and Komen et al. (1984). The wind input term is

$$S_{in}(f,\theta) = \max\left[0, 0.25\frac{\rho_a}{\rho_w}\left(\frac{u_5}{c}\cos(\theta-\theta_w)-1\right)\right]\omega F(f,\theta) \quad [10]$$

where ρ_a and ρ_w are the density of air and water, respectively, $c = \omega/k$ is the wave phase velocity, $F(f,\theta)$ is the frequency-directional spectrum. Again, without directly measuring c, we assume it is the same as that under the ice cover, i.e. ω/k_r, where k_r is calculated based on the viscoelastic model, θ_w is the corresponding mean wind direction. u_5 is the wind speed at 5m above the mean sea level, estimated by a simple logarithmic formula (Mears et al., 2001), i.e. $u_5 = \ln\left(\frac{5/z_0}{z_m/z_0}\right)u_{buoy}$, where z_0 is the roughness length, u_{buoy} is the wind speed measured at the measurement height z_m = 0.9m above the surface by instrument installed in the buoy (Thomson, 2012). Without direct measurement, z_0 is set as 0.0002 for open sea.

The dissipation term is

$$S_{ds}(f,\theta) = C_{ds}\hat{\omega}\frac{k}{\hat{k}}\left(\frac{\hat{\alpha}}{\hat{\alpha}_{PM}}\right)^2 F(f,\theta) \quad [11]$$

where C_{ds} is a constant ($C_{ds} = -2.36\times10^{-5}$), $\hat{\alpha}_{PM}$ is the value of $\hat{\alpha}$ for a Pierson–Moskowitz spectrum ($\hat{\alpha}_{PM} = 3.02\times10^{-3}$), $\hat{\omega} = \left(\overline{\omega^{-1}}\right)^{-1}$, $\hat{\alpha} = E\hat{k}^2 g^{-2}$, $\hat{k} = \left(\overline{1/\sqrt{k}}\right)^{-2}$, where the spectral average of a variable z is defined as $\bar{z} = \frac{\int_0^{2\pi}\int_0^{\infty} zF(f,\theta)dfd\theta}{\int_0^{2\pi}\int_0^{\infty} F(f,\theta)dfd\theta}$. The coefficients are provided by the WAVEWATCH III® user manual.

Nonlinear wave-wave interaction source term S_{nl} is calculated using Discrete Interaction Approximation (DIA, Hasselmann et al., 1985).

$$\begin{pmatrix}\delta S_{nl,1}\\ \delta S_{nl,3}\\ \delta S_{nl,4}\end{pmatrix} = D\begin{pmatrix}-2\\1\\1\end{pmatrix}C_{nl}g^{-4}f_{r,1}^{11}\left[F_1^2\left(\frac{F_3}{(1+\lambda_{nl})^4}+\frac{F_4}{(1-\lambda_{nl})^4}-\frac{2F_1F_3F_4}{(1-\lambda_{nl}^2)^4}\right)\right] \quad [12]$$

where $F_i = F(f_i,\theta_i)$ and $\delta S_{nl,i} = \delta S_{nl}(f_i,\theta_i)$, i=1, 3, 4. The two constants are: λ_{nl} = 0.25, $C_{nl} = 1.0\times10^7$ (Tolman and Chalikov, 1996).

6. Results

We selected 4 cases from 3 wave array experiments as shown in Table 1. Each case is composed of simultaneous data from two selected buoys. Attenuation rate against frequency $\alpha(f)$ is derived in each case as described in section 3. As shown in Fig. 1 (red dots), all of them show a rapid rise with increasing wave frequency up to a point, and then appear to plateau at very high frequencies.

Comparisons between the measured α and model results against angular frequency $\omega(=2\pi f)$ are shown in Fig. 1, with corresponding G, ν values summarized in Table 2. There is reasonably good agreement between data and models with calibrated G, ν. The difference of the results

between the simple model and the full model is mainly from wind input term S_{in}, which is affected by both wind direction and wind speed. For example, Fig. 1(b) shows some difference between two models at high frequencies. This is because waves in this range propagate in a similar direction as the wind. For high wind condition, i.e. case 4, the results in Fig. 1(d) show that the attenuation given by the full model is negative near angular frequency ω = 1.3Hz due to the strong wind effect. In all cases, S_{ds} is at least one order of magnitude less than other terms.

Table 1. Summary of the cases.

Case No.	Date (UTC)	Buoys No.	Ice concentration C	Ice thickness h (m)	Estimated wind speed $\boldsymbol{u_5}$ (m/s)
1	Oct. 4, 14:00 - 15:00	14 to 11	1	1	6.39
2	Oct. 18, 04:00 - 06:00	15 to 11	0.3	0.1	4.10
3	Oct. 31, 22:00 - 24:00	15 to 13	0.8	0.1	3.88
4	Nov. 1, 03:00 - 05:00	15 to 13	0.6	0.1	9.35

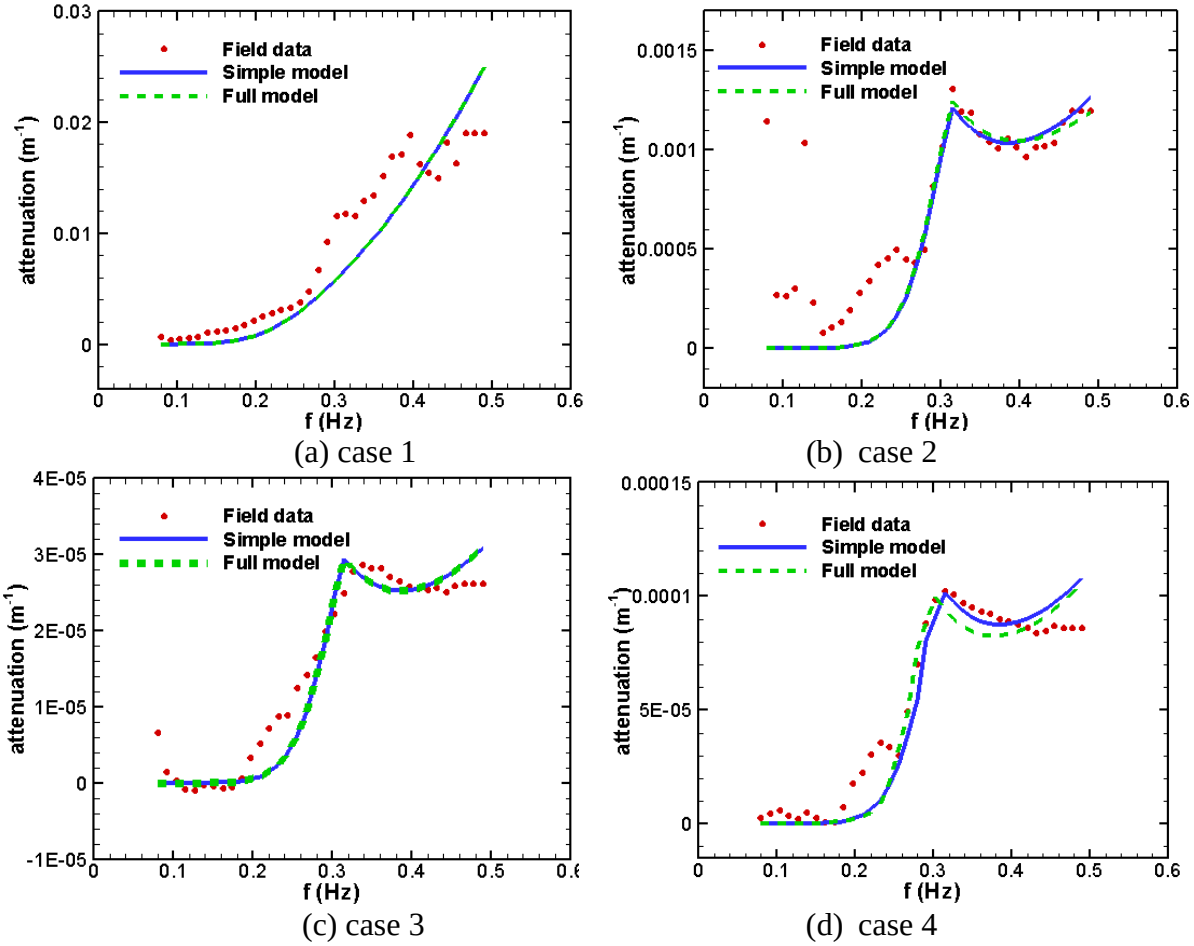

Figure 1. Comparison of attenuation calculated from models and data.

Table 2. Calibrated rheological parameters G, ν.

Case No.	Simple model		Full model	
	G (Pa)	ν (m^2/s)	G(Pa)	ν (m^2/s)
1	6989	0.3155	6989	0.3155
2	6000	0.13	6230	0.1545
3	6233	0.0013	6233	0.013
4	6326	0.0063	6683	0.076

7. Summary

A viscoelastic model that synthesized three classic sea ice models is calibrated using data from a recent field experiment. We consider two wave energy balance conditions. One assumes ice damping is the only mechanism, which is probably suitable for calm wave conditions. Under stormy conditions, the full energy balance equation including wind, wave dissipation, and nonlinear transfers are considered. We use these two energy balance equations and an optimization method to determine the best-fit rheological parameters in the viscoelastic model. It is found that a reasonable fit can be obtained for most of the frequency range.

The results presented are preliminary. Both the wave and the ice data are going through further analysis. Modifications of the calibration will be conducted as these new and improved data become available. The completed product of this calibration effort will then be available for wave models to predict wave conditions under similar ice covers.

Acknowledgments

This work is supported by the Office of Naval Research Grant #N00014-13-1-0294 (Shen); N0001413WX20825 (Rogers); N000141310284 (Thomson).

Reference

De Carolis, G., and Desiderio, D., 2002. Dispersion and attenuation of gravity waves in ice: a two-layer viscous fluid model with experimental data validation. Phys. Lett. A, 305(6):399-412.

Fox, C., and Squire, V.A., 1994.On the oblique reflexion and transmission of ocean waves at shore fast sea ice. Phil. Trans. Royal Soc. London A: Math. Phys. Eng. Sci., 347(1682):185-218.

Hasselmann, S., Hasselmann, K. Allender, J.H. and Barnett, T.P., 1985. Computations and parameterizations of the nonlinear energy transfer in a gravity-wave spectrum, Part II: parameterizations of the nonlinear energy transfer for application in wave models. J. Phys. Oceanogr., 15:1378-1391.

Komen, G.J., Hasselmann, S., and Hasselmann, K., 1984.On the existence of a fully developed wind-sea spectrum. J. Phys. Oceanogr., 14:1271–1285.

Keller, J.B., 1998. Gravity waves on ice-covered water. J. Geophys. Res.–Oceans, 103(C4):7663-7669.

Li, J., Kohout, A.L., and Shen, H.H., 2015. Comparison of wave propagation through ice covers in calm and storm conditions. Geophys. Res. Lett., 42(14):5935-5941.

Lygre, A., and Krogstad, H.E., 1986. Maximum entropy estimation of the directional distribution in ocean wave spectra. J. Phys. Oceanogr., 16(12):2052-2060.

Mears, C., Smith, D., and Wentz, F.J., 2001. Comparison of SSM/I and buoy-measured wind speeds from 1987–1997. J. Geophys. Res.–Oceans, 106(C6):11719–11729.

Mosig, J.E., Montiel, F., and Squire, V.A., 2015. Comparison of viscoelastic-type models for ocean wave attenuation in ice-covered seas. J. Geophys. Res.–Oceans, 120(9):6072-6090.

Snyder, R.L., Dobson, F.W., Elliott, J.A., and Long, R.B., 1981. Array measurements of atmospheric pressure fluctuations above surface gravity waves. J. Fluid Mech., 102:1-59.

Thomson, J., 2012. Wave Breaking Dissipation Observed with “SWIFT” Drifters. J. Atmos. Oceanic Technol., 29:1866–1882, doi: http://dx.doi.org/10.1175/JTECH-D-12-00018.1.

Thomson, J., and Rogers, W.E., 2014. Swell and sea in the emerging Arctic Ocean. Geophys. Res. Lett., 41(9):3136-3140.

Tolman, H.L., and the WAVEWATCH III® Development Group, 2014. User manual and system documentation of WAVEWATCH III® version 4.18. Tech. Note 316, NOAA/NWS/NCEP/MMAB.

Tolman, H.L., and Chalikov, D., 1996. Source terms in a third-generation wind wave model. J. Phys. Oceanogr, 26(11): 2497-2518.

Wadhams, P.,1986. The seasonal ice zone. In The geophysics of sea ice, 825-991.Springer US.

Wang R., Shen H.H., 2010. Gravity waves propagating into an ice-covered ocean: A viscoelastic model. J. Geophys. Res.–Oceans, 115(C6), doi: 10.1029/2009JC005591.

Zhao, X., and Shen, H.H., 2015. Ocean wave transmission and reflection by viscoelastic ice covers. Ocean Modelling, 92:1-10.